



UDK / UDC 620

Izvorni znanstveni članak / Original scientific paper

Prihvaćeno / Accepted: 20. 3. 2014.

STRUCTURES AND MICROHARDNESS OF PINNA PECTINATA SEASHELL'S

Tomislav Filetin, Irena Žmak*

University of Zagreb, Faculty of Mechanical Engineering and Naval Architecture

Abstract

The natural structures and materials offer an inspiration for new solutions in the development of advanced engineering cellular and composite materials. The lamellar nacreous (mother of pearl), cross-lamellar and prismatic structures of seashells are especially interesting for development of the biomimetic concepts of nano- and micro- laminate composites.

The inner surface layer of narrower part the *Pinna pectinata* (*Pinnidae*) shell has a nacreous structure composed of aragonite platelets surrounded with an organic phase and in the outer layer a polygonal prismatic structure with high ratio length/thickness of columns. The whole cross-section of the upper wider shell part constitutes of the polygonal columnar crystals surrounded with an organic phase as well.

Nano- and micro-indentation gives valuable information about the mechanical behaviours particularly by compression, but also by tensile and shear load.

The Vickers microhardness of *Pinna pectinata* (*Pinnidae*) Adriatic Sea mollusc shells structure has been determined as a function of the indentation load and loading direction. The load dependence of microhardness is analyzed by using the known Meyer's law and modified proportional specimen resistance (PSR) model. The best correlation between measured values and used models is achieved by using the modified PSR model.

The results show that the measured microhardness depends on the load for the lamellar and prismatic structures, except for the prismatic ones indented perpendicularly to the outer surface.

Key words: microhardness; indentation size effect (ISE); seashell structures

* Department of Materials, I. Lučića 5, HR-10000 Zagreb, Croatia, tfiletin@fsb.hr, irena.zmak@fsb.hr



1. INTRODUCTION

The seashells are composed of ductile organic and brittle inorganic phases and they are hierarchically structured at nano-, micro-, meso-levels [1,2]. These complex structures are inspiring materials scientists in the design of mimetic processes for synthesis of advanced multilayer nano-laminate and other particle composite materials [3-10].

Nano- and micro-indentation is simple to be carried out and gives valuable information about mechanical response under compression but also under tensile and shear load. A lot of results for the indentation size effect (ISE) for ceramic materials [11-15] exist, but not many are available for such kind of biological organic/inorganic composites. From the nano-indentation testing [16,17] for different seashell structures it could be assumed that in micro-scale a similar effect exists. Some research has already been done by the authors of this paper [18-20].

In this investigation the Vickers microhardness of species *Pinna pectinata* from the Adriatic Sea (Class: *Bivalvia*, Order: *Mytiloidea*, Family: *Pinnidae*) mollusc shells structures of narrower part at inner and outer surface (Fig. 1a) has been determined as a function of the indentation load and loading direction. This mollusc shell is a large (30-48 cm long), triangular, thin, brittle shell tapering to a point (Fig. 1a). Fan-mussels live with their pointed end embedded in sediment, attached by abundant fine byssal threads to pebbles and shell fragments. Inside of the shell it is glossy, partly lamellar in bottom part where the mussel lives.

2. SHELL STRUCTURE

All of the mollusc seashell structures have the typical biological composite structures with various distributions and organizations of hard and soft components. The possible types of mollusc shell materials and structures are: prismatic, lamellar, crossed-lamellar, foliated and homogeneous (Table 1).

The adequate combination of strength and ductility results in high energy absorption prior to failure. The most common mineral components are calcium carbonate, calcium phosphate (hydroxyapatite), and amorphous silica. Altogether there are more than 20 different minerals in sea mollusc shells. These minerals are embedded in a complex assemblage of organic macromolecules of keratin, collagen, and chitin that are hierarchically organized [21]. The values of the mechanical properties of various structures are quite dependent on the mode of loading due to structural anisotropies [22-24].

2.1 Results of microstructural analysis

Two dry shell samples (Fig. 1a) have been analysed by the scanning electron microscope (Figures 1b, 2 and 3). The first sample was taken from the lower part of the sea shell

Table 1 – Types of mollusc shell materials and structures [2]**Tablica 1** – Vrste materijala i struktura oklopa školjaka [2]

Type	Shape	Crystal		Protein matrix, wt%	Mean strength, MPa			Stiffness (Modulus of elast.), GPa	Vickers hardness, HV
		C	A		R_m	R_c	R_b		
Prismatic	Columnar 0.1 μm by few μm	Y	Y	1-4	60	250	140	30	162
Lamellar-Nacreous	Flat platelets: 0.3-0.8 μm thick	N	Y	1-4	130	38	220	60	168
Crossed-lamellar	Plywood-like lamella 20-40 μm thick	N	Y	0.01-4	40	250	100	60	250
Foliated	Long, thin crystals in overlapping layers	Y	N	0.1-0.3	30	150	100	40	110
Homogeneous	0.5-3 μm diameter	N	Y	Very tenuous	30	250	80	60	–

C = calcite, A = aragonite, Y/N = yes/no, R_m = tensile, R_c = compressive, R_b = bending

(Position A, as in Fig. 1.a), which is where the mussel itself lives. The second sample was taken at the Position B (Fig. 3. b), i.e. in the upper, wider part of the shell.

The micrograph analysis at Position A has shown that the structure of the inner shell surface is lamellar nacreous “mother of pearl” (i.e. with aragonite platelets), surrounded with the organic phase (Fig. 2). The thickness of each aragonite platelet is about up to 0.5 μm , and the whole nacreous layer has an average thickness of 60 to 200 μm .

On the other hand, the outer surface consists of regularly arranged pentagonal or hexagonal prisms (columnar structure), also surrounded with the organic phase (Fig. 1b).

When the seashell structure was analysed at Position B, as shown in Fig. 1.a, it was found that here the seashell consists only of regular columnar crystals (Fig. 3 and 6b). As in Position A, the columnar crystals are either pentagonal or hexagonal, see Figures 4a and 4b. These crystals have the thickness of up to 50 μm and an average length of 500 to 900 μm .

This honeycomb-like structure has a very high length-to-thickness ratio, and also the highest ratio between the surrounding area and the cross-section area of each column. This indicates that the great surrounding areas consist out of organic phase, which is responsible for the elastic behaviour of the seashell structure. This duplex structure

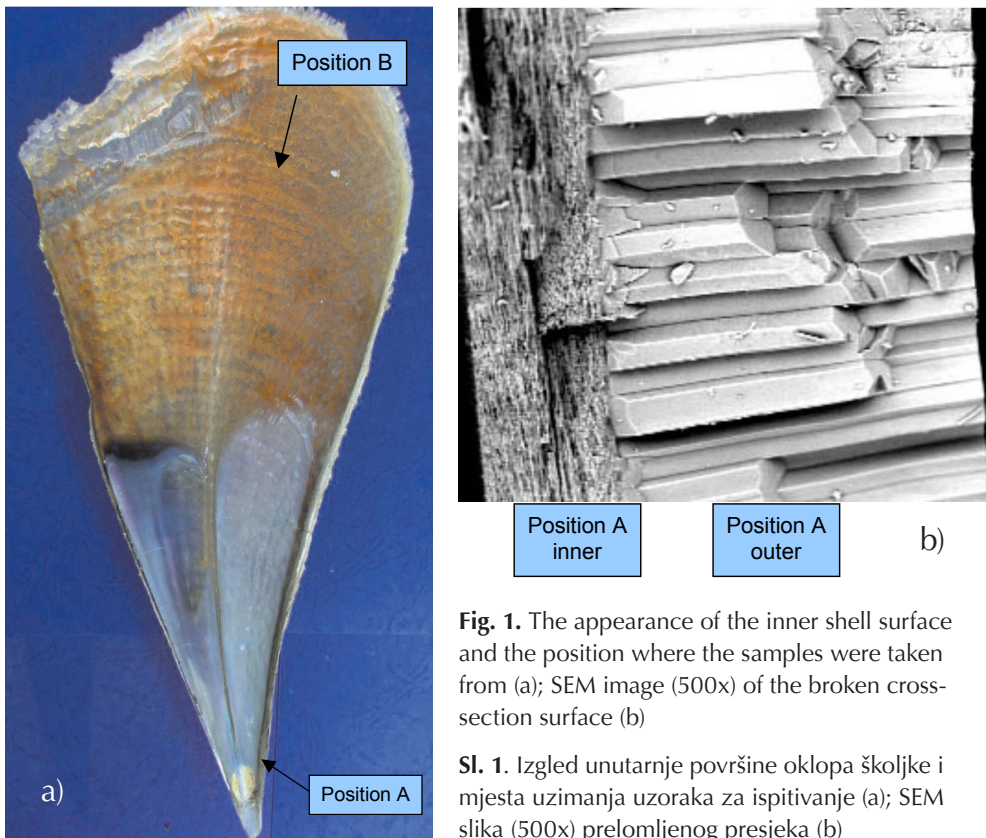


Fig. 1. The appearance of the inner shell surface and the position where the samples were taken from (a); SEM image (500x) of the broken cross-section surface (b)

Sl. 1. Izgled unutarnje površine oklopa školjke i mjesta uzimanja uzoraka za ispitivanje (a); SEM slika (500x) prelomljenog presjeka (b)

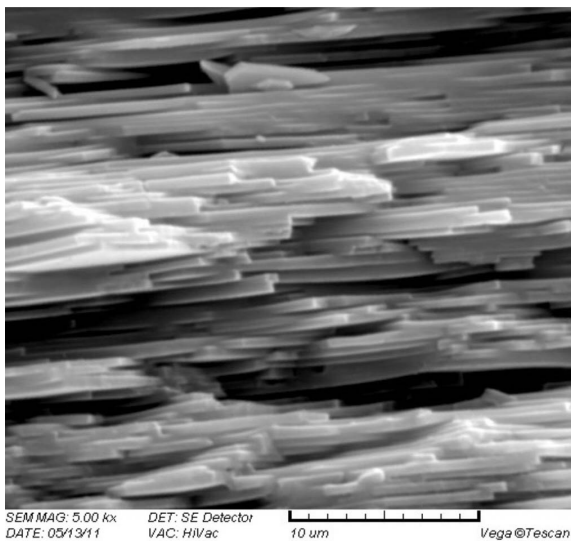


Fig. 2. SEM image shows the nacreous (mother of pearl) structure of the inner shell layer, as observed on the broken cross-section at the Position A

Sl. 2. SEM snimka prikazuje lamelarnu strukturu unutarnje površine na prelomljenom presjeku na poziciji A

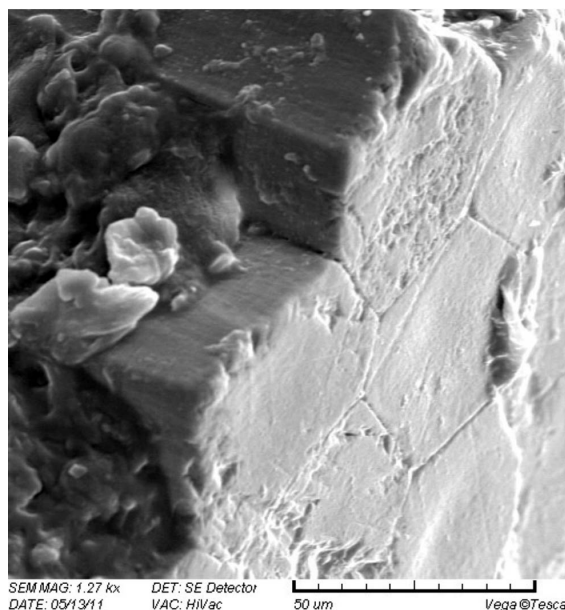


Fig. 3. SEM image of the prismatic structure observed at the broken cross-section at the Position B

Sl. 3. SEM snimka prizmatične strukture analizirane na prelomljenoj površini presjeka na poziciji B

indicates the functionally gradient properties of the composite. For this reason, it is assumed that the seashell's mechanical resistance to compression perpendicular to the inner and outer surface will be quite different.

Fig. 3 and Fig. 4 show quite regular polygonal arrangements of the columns.

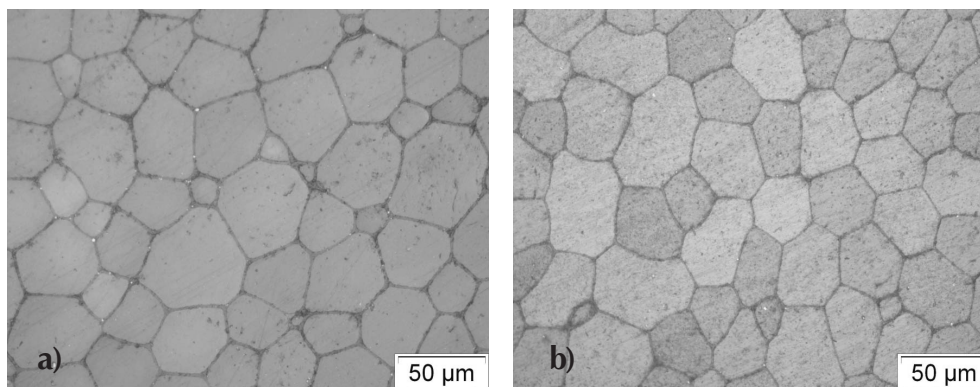


Fig. 4. Optical micrographs of the inner (a) and outer surface (b) of the prismatic structure at the Position B (550x) after grinding and polishing

Sl. 4. Optičke mikrografske snimke unutarnje (a) i vanjske površine (b) prizmatične strukture na poziciji B (550x) nakon brušenja i poliranja

3. HARDNESS MEASUREMENT METHODS

The purpose of hardness testing was to determine the indentation micro size effect (ISE) and to analyse the other phenomena after compression loading of the shell structures.

The ISE can schematically be represented as the dependence between the hardness and the indentation load (Fig. 5).

The testing of ceramics or single crystals has confirmed that the hardness is usually dependent [11-15] on the increase in the applied load.

The Meyer's law [26] is simply an empirical expression used to describe the relationship between the indentation load (F) and the resultant indentation size, i.e. Vickers indentation diagonal (d):

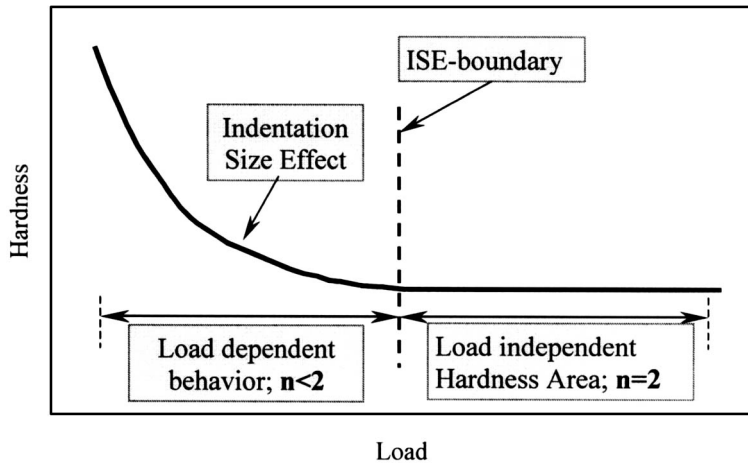


Fig. 5. Schematic dependence between hardness and indentation load (ISE) [25]

Sl. 5. Shematski prikaz ovisnosti tvrdoće i opterećenja (ISE) [25]

$$F = kd^n \quad (1)$$

where k is the constant for a given material or structure and n is the Meyer's index, which is a measure of the ISE. Index n for metals is roughly related to the strain-hardening coefficient in the exponential equation for the true stress-strain curve.

An alternative analysis of the ISE to the Meyer's law is the proportional specimen resistance model (PSR), and recently a number of researches have explained the ISE with this model. Li and Bradt [27] have introduced the proportional specimen resistance model (PSR). In this model, the applied test load (F), and the resulting indentation diameter size (d), were found to follow the relationship:

$$F = a_1 \cdot d + a_2 \cdot d^2 \quad (2)$$

where a_1 and a_2 were considered as constants and can be related to elastic and/or plastic properties of the tested materials, respectively. Coefficient a_2 (N/mm²) should be a measure of load-independent hardness, or so-called 'true' hardness. Equation (2) can be transformed into:

$$F/d = a_1 + a_2 \cdot d \quad (3)$$

The parameters a_1 and a_2 from equation (3) are evaluated through the linear regression of F/d versus d . The dependence of F/d versus d is linear, with the line slope equal to the a_2 parameter and the intercept equal to the value of the a_1 parameter.

The modified PSR model has been designed by Gong et al. [28] on the basis of the consideration of the effect of a machining-induced, residually stressed surface on the hardness measurements, giving:

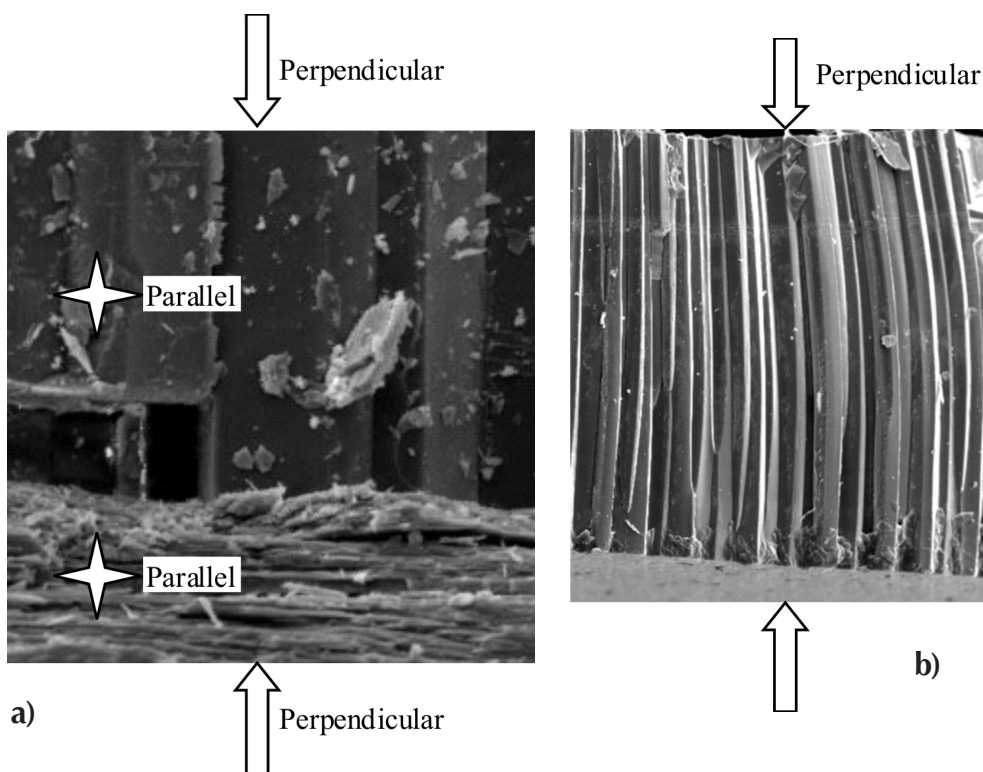


Fig. 6. The loading directions at the Position A (a) and at the Position B (b)

Sl. 6. Smjerovi opterećivanja na poziciji A (a) i na poziciji B (b)

$$F = F_0 + a_1 \cdot d + a_2 \cdot d^2 \quad (4)$$

where F_0 is a constant related to the surface residual stresses associated with the surface machining and polishing, while a_1 and a_2 are the same parameters as in equation (2).

The Vickers microhardness values of two different seashells structures, one on the inner and the other on the outer shell surface, both taken from the Position A, have been determined as a function of the indentation load and indentation direction.

The characteristic applied loading directions were: parallel to the inner and outer surface (i.e. normal to the broken cross-section), and perpendicular to the inner and outer surface (Fig. 6a).

Additionally, the measurements have been performed by loads up to 49.5 N at the Position B, perpendicular to the inner at outer surface (Fig. 6b).

The cross-sections of the samples were prepared by the standard ceramographic technique: cutting by a ceramic plate, cold casting in resin at ambient temperature, progressive grinding, polishing with diamond suspension and DP-Lubricant Blue. The small and quite flat samples have additionally been only cold cast. These samples have been used for hardness indentation perpendicular to the inner and outer surface. Vickers hardness measurements HV0.1, HV0.2, HV0.5, and HV1 were performed using the indentation loads of 0.9807 N, 1.961N, 4.903 N, and 9.81 N, all with the loading duration of 15 s. Indentation tests were carried out under ambient laboratory conditions on the Instron Wilson-Wolpert Tukon 2100B Hardness Tester.

Eight indentations for each load were performed at each prepared sample, and the average values of these have been calculated for further statistical analysis.

4. RESULTS AND DISCUSSION

If loading has been applied perpendicularly to the outer surface around the indentations, the quite different zones at the Position A have been found in comparison to such zones at the Position B (Fig. 7). At the Position A the structure collapse (i.e. brittle crushing) was observed at the indentation edges (Fig. 7a). SEM analysis of the indentation at the Position B showed the splitting in the longitudinal direction of the prisms, due to shear stresses (Fig. 7b).

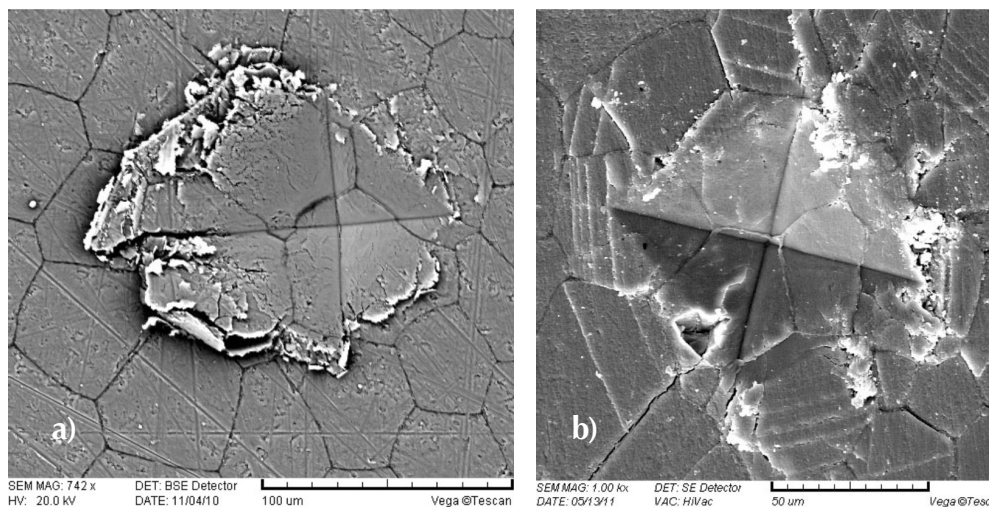
Determined parameters according to Meyer's law for the samples taken from the Position A are presented in Table 2.

For all samples the calculated Meyer's index n is below 2, therefore the hardness is dependent on applied load. The exception is the outer layer with indentation applied perpendicularly to the shell surface, where the index is greater than 2; therefore the hardness here is independent on applied load.

The values of k indicate a different response of structures at indentation. Correlation coefficients of Mayer's law are very high for all tested samples.

Table 2 – Regression analysis of measured data for the Position A, according to equation (1)**Tablica 2** – Regresijska analiza izmjerenih podataka za poziciju A prema jednadžbi (1)

Sample	n	k, N/mm ⁿ	Coeff. of determination R ²
A-In-Parallel	1.845	868.36	0.999
A-Out-Parallel	1.618	374.02	0.996
A-In-Perp.	1.443	299.43	0.998
A-Out-Perp.	2.062	1416.77	0.999

**Fig. 7.** SEM images of the indentations perpendicular to the outer surface at the Position A (a) and at the Position B (b), using indentation load 0.98 N

Sl. 7. SEM snimke utisnuća okomito na vanjsku površinu na poziciji A (a) i na poziciji B (b) uz opterećenje od 0,98 N

The relationships between the microhardness of the different structures and applied loads are drawn in Fig. 8. Results show that the microhardness decreases with the increasing indentation load according to the power laws with very high regression coefficients, except for the outer layer by indentation applied perpendicularly where the hardness is load-independent.

With the indentation direction parallel to the inner shell surface, the lamellar structure showed higher hardness values than the prismatic one.

Furthermore, applying the indentation perpendicularly to the inner surface, the lamellar structure exhibited a significantly higher hardness than in the case of loading parallel to the same surface.

The hardness with the application of higher indentation loads (up to 49.5 N) was also measured. Fig. 9 compares the measured hardness in dependence of the applied

load for the prismatic seashell structure, while loading perpendicular to shell surface at Positions A and B. At Position A (Sample A-Out-Perp.) the measurements were made at the outer shell surface. On the other hand, the results on Fig. 9 presented for the sample B-In&Out-Perp. are the mean values between values obtained at the inner and outer seashell surface.

Since the sample A-Out-Perp. has a lamellar base, which acts as a support for the columns, this sample exhibits greater hardness when loading perpendicularly to the columns than the sample B-In&Out-Perp (Fig. 9). This sample was taken from the Position B, where only columnar crystals without any nacre were observed.

The hardness measured with higher indentation loads also indicates the presence of the indentation size effect of this columnar structure, too, as shown in Table 3. The logical explanation for this effect would be that the indentation with higher loads affects a greater number of columns than with lower loads, and therefore involves also a higher rate of organic surrounding phase, which consequently decreases the hardness.

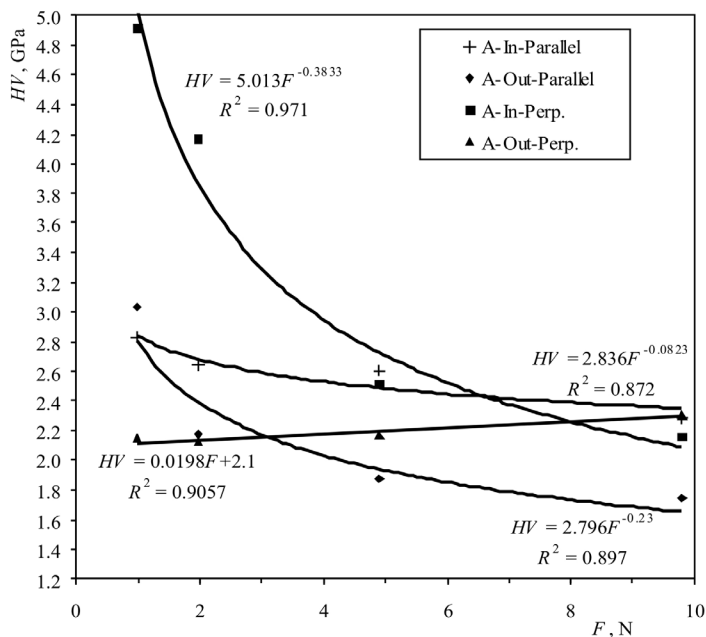
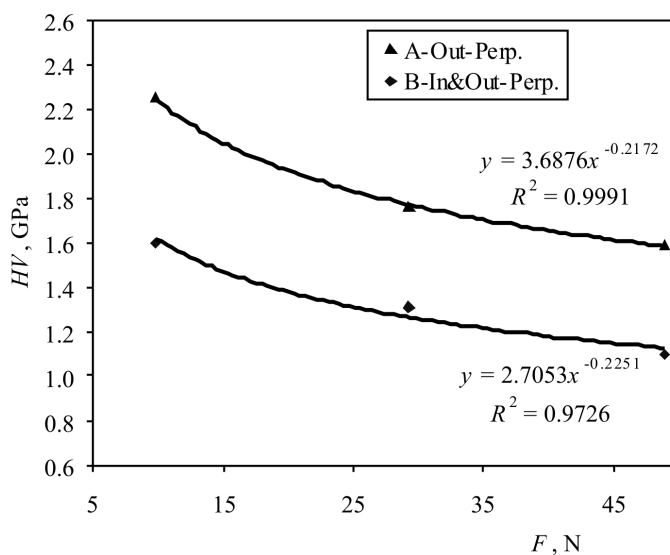


Fig. 8. Measured hardness in dependence to the applied load for the lamellar and prismatic structures and for two loading directions, all measured at the Position A

Sl. 8. Izmjerene tvrdoće u ovisnosti o opterećenju za sedefastu i prizmatičnu strukturu, za dva smjera opterećivanje, sve mjereno na poziciji A

Table 3 – Regression analysis of experimental data according to equation (1) for the higher applied loads**Tablica 3** – Regresijska analiza eksperimentalnih podataka prema izrazu (1) za veća opterećenja

Sample	n	k, N/mm ⁿ	Coeff. of determination R ²
A-Out-Perp.	1.7705	536.66	0.997
B-In&Out-Perp.	1.4364	246.77	0.984

**Fig. 9.** Measured hardness in dependence to the higher applied load for the prismatic structure, perpendicular to the shell surface at the Positions A and B

Sl. 9. Izmjerene vrijednosti tvrdoća u ovisnosti o većim opterećenjima za prizmatičnu strukturu, okomito na vanjsku površinu (pozicija A), te okomito na vanjsku i unutarnju površinu (pozicija B)

Fig. 10 and 11 illustrate the relationship between the load F and indentation diagonal size d for the tested seashell samples taken from the Position A, according to the modified PSR model. The curves in these plots are obtained by polynomial laws, all with very high correlation coefficients.

The load-independent hardness has also been referred to as the 'true' hardness (HV_0) in some literature. The true Vickers hardness could be calculated by the following equation from [15]:

$$HV_0 = 1.8544 \cdot a_2 \quad (5)$$

where a_2 is the coefficient from the equation (3).

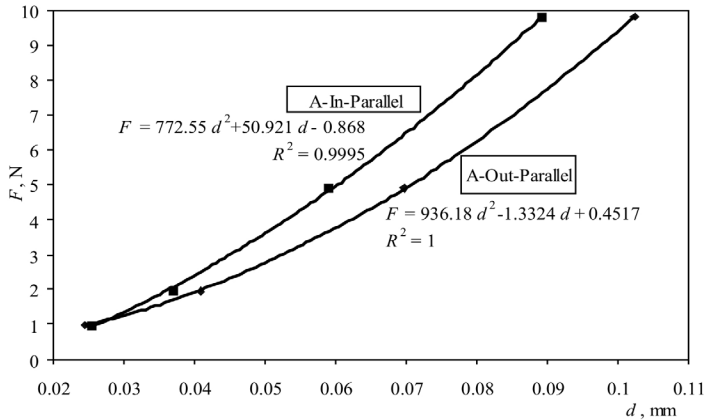


Fig. 10. The applied load vs. indentation size according to the modified PSR model for indentation parallel to the shell surfaces, at the Position A

Sl. 10. Ovisnost primijenjenog opterećenja i veličine otiska prema modificiranom PSR modelu, za utisnuća paralelno s površinama na poziciji A

PSR model gives the coefficients (a_1, a_2) from the equation (3) and the true hardness values (HV_0) according to the equation (5), see Table 4.

The data in Table 4 show that at the lower part of the seashell (Position A) the highest true hardness value exhibits the polygonal crystal prismatic structure, when

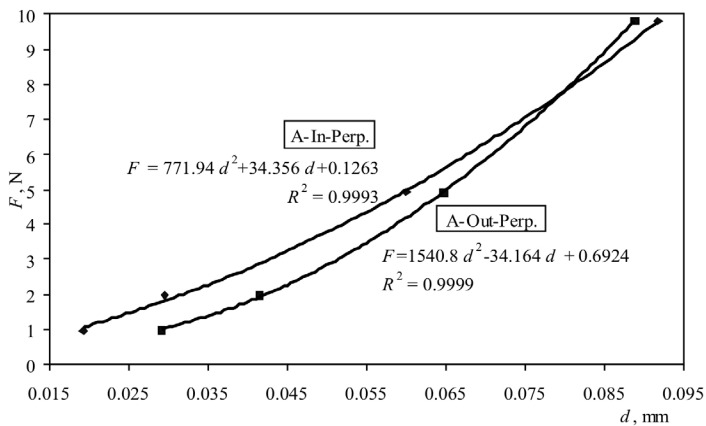


Fig. 11. The applied load vs. indentation size according to the modified PSR model for indentation perpendicular to the inner and outer surface, at the Position A

Sl. 11. Ovisnost primijenjenog opterećenja i veličine otiska prema modificiranom PSR modelu, za utisnuća okomito na unutarnju i vanjsku površinu na poziciji A

loaded perpendicular to the outer seashell surface. The underlying lamelled layer acts here as an elastic substrate.

Table 4 – The coefficients from the PSR model and the true hardnesses for the Position A

Tablica 4 – Koeficijenti iz PSR modela i stvarne vrijednosti tvrdoća na poziciji A

Sample	a_1	a_2	HV ₀ , GPa
A-In-Parallel	11.89	1125.5	2.09
A-Out-Parallel	20.21	730.24	1.35
A-In-Perp.	40.33	719.67	1.33
A-Out-Perp.	5.19	1286.50	2.39

5. CONCLUSION

The both investigated lamellar and columnar seashell structures show the indentation micro-size effect in both parallel and perpendicular indentation directions. The exception is the prismatic crystal structure with the lamellar substrate when indented perpendicular to the outer seashell surface. In this case the hardness is load-independent in the range from 0.981 to 9.81 N.

The hardness measurements with application of higher indentation loads (up to 49.5 N) indicate the presence of indentation size effect of this columnar structure, too. The indentation with higher loads affects more columns than with lower loads, and therefore involves also a higher rate of organic surrounding phase, which consequently decreases the hardness.

The seashell is harder where the columnar crystals have the lamellar base underneath them, since the nacre acts as a support for the columns.

Meyer's law has proved to be satisfactory for the description of experimental data with very good correlation.

The best correlation between the indentation load and the resulted diameter (hardness) values has been achieved by using the modified PSR model.

The hardness in perpendicular direction to the inner surface (lamellar aragonite structure) is higher than by loading parallel to the same surface (i.e. perpendicular to the cross-section). In the perpendicular direction the harder aragonite platelets crushed under prevailing normal stress without any larger inter-lamellar sliding, or in other words without plastic deformation. On the other hand, while loading at the cross section parallel to the inner surface the organic phase gives certain plasticity to the seashell, so the platelets slide more before cracking.

The columnar structure shows a specific behaviour when compressed in longitudinal direction, which will need further explanation based on mechanics of similar forms in composite structures. At higher applied loads the hardness is lower, since the indentati-

on affects a greater number of columns. More columns mean a higher relative content of the organic phase, which is responsible for lamellar sliding. Especially interesting would be the explanation of the behaviour of the combined lamellar/prismatic structure.

The forthcoming investigations will be directed towards the design, manufacturing and testing of such composite structures, which have similar constituent forms like those observed in the investigated seashell.

Acknowledgments

This research was founded by the University of Zagreb – project No 10206-2.

The authors would like to thank Suzana Jakovljević, PhD and Sanja Šolić, PhD for microstructure and hardness measurements.

References

- [1] J. D. Currey: Mechanical Properties of Mollusc Shell; Symposia of the Society for Experimental Biology, Cambridge University Press, 1980.
- [2] G. Mayer, M. Sarikaya: Rigid Biological Composite Materials: Structural Examples for Biomimetic Design, *Experimental Mechanics*, Vol. 42 (No4), Dec. 2002. pp. 395-403.
- [3] M. Sarikaya, H. Fong, J. M. Sopp, K. S. Katti, G. Mayer: Biomimetics: Nanomechanical Design of Materials through Biology; 2002, in the Proc. of the 15th ASCE Eng. Mechanics Conf. Columbia University, New York.
- [4] P. Calvert, J. Cesarano, H. Chandra, H. Denhim, S. Kasichainula, R. Vaidyanathan: Toughness in Synthetic and Biological Multilayered Systems; *Phil. Trans. R. Soc. London A360*, (2002), pp. 199-209.
- [5] A. A. Abdala, D. L. Milius, D. H. Adamson, I. A. Aksay, R. K. Prud'homme: Inspired by Abalone Shell: Strengthening of Porous Ceramics with Polymers; *Science and Eng.* 90, (2004), pp. 384-385.
- [6] K. S. Vecchio: Synthetic Multifunctional Metallic-Intermetallic Laminate Composites, *JOM*, 2005 (3), p. 57.
- [7] F. A. Burgman, X. L. Xaio, D. G. McCulloch, D. R. McKenzie, M. M. M. Bilek, B. K. Gan, L. Ryves: Relationship Between Microstructure, Stress and Hardness in Multi-layer Coatings, *Micros Microanal* 11 (Suppl 2), 2005.
- [8] G. Mayer: New classes of tough composite materials - Lessons from natural rigid biological systems, *Materials Science and Engineering C* 26 (2006), pp. 1261-1268.
- [9] P. Podsiadlo, Z. Liu, D. Paterson, P.B. Messersmith, N.A. Kotov: Fusion of Seashell Nacre and Marine Bioadhesive Analogs: High-Strength Nanocomposite by Layer-by-Layer Assembly of Clay and L-3,4-Dihydroxyphenylalanine Polymer, *Adv. Mater.* 2007, 19, pp. 949-955, DOI: 10.1002/adma.200602706.

- [10] R. Narayanan, S. Dutta, S. K. Seshadri: Hydroxy apatite coatings on Ti-6Al-4V from seashell, *Surface & Coatings Technology* 200 (2006), pp. 4720-4730.
- [11] J. Gong, Z. Guan: Load dependence of low-load Knoop hardness in ceramics: a modified PRS model, *Mater. Lett.*, 47 (2001) 140-144.
- [12] X. J. Ren, R. M. Hooper, C. Griffiths, J. L. Henshall: Indentation size effect in ceramics: correlation with H/E, *J. Mater. Sci. Lett.*, 22 (2003), pp.1105-1106.
- [13] J. Gong, J. Wu, Z. Guan: Examination of the indentation size effect in low-load Vickers Hardness testing of ceramics, *J. Eur. Ceram. Soc.* **19** (1999), pp. 2625-2631.
- [14] M. Lalić, L. Čurković: Analysis of the ISE on hardness of CIP-Al₂O₃ ceramics using different models, in *Proc. of the 3rd Inter. Conf. on Modeling, Simulation and Applied Optimization*, Sharjah, U.A.E, Jan. 20-22. 2009.
- [15] J. Andrejovska, J. Dusza: Hardness and Indentation Load/Size Effect in Silicon based Ceramics, in *Proc. of the NANOCON 2009*, Rožnov pod Radhoštěm, Czech Rep., 6p.
- [16] F. D. Fleischli, M. Dietiker, C. Borgia, R. Spolenak: The influence of internal length scales on mechanical properties in natural nanocomposites: A comparative study on inner layers of seashells, *Acta Biomaterialia* Vol. 4, Issue 6, pp. 1694-1706, Nov. 2008.
- [17] H. M. Leung, S. K. Sinha: Scratch and indentation test on seashells, *Tribology Inter.* 42(2009), pp. 40-49.
- [18] J. Šubarić, T. Filetin: Structure and Properties of Mollusc Shells, *MATRIB 08*, Vela Luka, 26-28.06 2008, (abstract, full text on CD pp. 362-367).
- [19] T. Filetin, I. Žmak, S. Šolić, S. Jakovljević: Microhardness of mollusc seashell structures, *Proceedings of Inter. Conf. on Innovative Technologies IN-TECH 2010*, Prague, 14-16. 09. 2010. pp. 95-97.
- [20] T. Filetin, S. Šolić, I. Žmak: The indentation size effect on the microhardness of sea mollusc shell structures, *Materials Testing* 53 (2011) 1-2, pp. 48-53.
- [21] M. A. Meyers, A. Y. M. Lin, Y. Seki, P. Chen, B. K. Kad, S. Bodde: Structural Biological Composites: An Overview, *JOM*, 2006.
- [22] R. Z. Wang et al.: Deformation Mechanisms in Nacre, *J. Mater. Res.*, 16, (2001), pp. 2485-2493.
- [23] A. G. Evans et al.: Model for the Robust Mechanical Behavior of Nacre, *J. Mater. Res.*, 16, (2001), pp. 2475-2484.
- [24] F. Barthelat, H. Tanga, P. D. Zavattieri, C.-M. Li, H. D. Espinosa: On the mechanics of mother-of-pearl: A key feature in the material hierarchical structure, *Journal of the Mechanics and Physics of Solids* 55 (2007), pp. 306-337.
- [25] S. Sebastian; M. A. Khadar: Microhardness indentation size effect studies in 60B₂O₃-(40-x)PbO-xMCl₂ and 50B₂O₃-(50-x)PbO-xMCl₂ (M=Pb, Cd) glasses, in: *J. Mater. Sci.* 40 (2205), pp. 1655-1659.
- [26] D. Tabor: *The Hardness of Metals*, Oxford University Press, Oxford, 1951.

- [27] H. Li, R. C. Bradt: The microhardness indentation load/size effect in rutile and cassiterite single crystals, *J. Mater. Sci.* 28 (1993), pp. 917-926.
- [28] J. Gong, J. Wu, Z. Guan: Examination of the indentation size effect in low-load Vickers hardness testing of ceramics, *J. Eur. Ceram. Soc.* 19 (1999), pp. 2625-2631.

Struktura i mikrotvrdoća oklopa školjke *Pinna pectinata*

S a ž e t a k

Prirodne strukture i materijali nude inspiracije za traženje novih rješenja u razvoju naprednih ćelijastih i kompozitnih inženjerskih materijala. Lamelarne, unakrsno-lamelarne i prizmatične strukture oklopa morskih školjaka su naročito zanimljive za biomimetičke koncepte razvoja nano i mikro laminatnih kompozita

Unutarnji površinski sloj užeg dijela oklopa školjke *Pinna pectinata* (periska) ima lamelarnu strukturu sastavljenu od aragonitnih pločica okruženih s organskom fazom, dok je na vanjskoj površini poligonalna prizmatična struktura s velikim omjerom duljina/debljina prizmi, okruženih također s organskom fazom. Gornji širi dio oklopa školjke po cijelom presjeku ima poligonalnu prizmatičnu strukturu.

Mjerenje tvrdoće u nano i mikro području opterećenja daje vrijedne informacije o mehaničkom ponašanju naročito u uvjetima tlačnog, ali i vlačnog te posmičnog opterećenja.

Mikrotvrdoća po Vickersu oklopa *Pinna pectinata* (*Pinnidae*) jadranske školjke periske određena je u ovisnosti o opterećenju pri utiskivanju za dva smjera utiskivanja. Ovisnost mikrotvrdoće o opterećenju analizirana je koristeći poznat Mayerov zakon i modificiran model proporcionalne otpornosti uzorka (PSR). Najbolja korelacija između mjerenih vrijednosti utvrđena je korištenjem modificiranog PSR modela.

Rezultati pokazuju da mjerena mikrotvrdoća ovisi o opterećenju za lamelarnu i prizmatičnu strukturu, izuzevši za opterećivanje okomito na vanjsku površinu prizmatičnih stupića.

Ključne riječi: mikrotvrdoća; efekt veličine utisnuća; strukture oklopa školjaka

Full Prof. Tomislav Filetin, PhD
University of Zagreb,
Faculty of Mechanical Engineering
and Naval Architecture,
Department of Materials

Assist. Prof. Irena Žmak
University of Zagreb,
Faculty of Mechanical Engineering
and Naval Architecture,
Department of Materials